Investigating the Life and Death of the Early Paleozoic Moyero River Geomagnetic Superchron: Middle Ordovician Paleomagnetism from Estonia

Thesis by

J. Michael Grappone, Jr

In Partial Fulfillment of the Requirements for the Degree of

Master of Science

CALIFORNIA INSTITUTE OF TECHNOLOGY

Pasadena, California

2016

ABSTRACT

Flat-lying Early and Middle Ordovician limestones exposed on the North margin of Estonia provide key insights into the early Paleozoic biosphere and climatic history of the Baltic Platform, and potentially offer a site for calibrating the duration of the proposed Moyero River Reversed Superchron. Past paleomagnetic analyses on these rocks have been focused primarily on determining paleomagnetic pole positions and have been hampered by relatively weak remanent magnetizations. We therefore applied techniques of the Rock and Paleomagnetic Instrument Development (RAPID) consortium using thin-walled, low-noise quartz glass sample holders on an automatic system to enhance magnetostratigraphic resolution. Our results, based on over 300 oriented core samples spanning the stratigraphic interval from the Volkhov stage, up through the Lasnamägi stage, confirm previous work isolating a stable characteristic magnetization of reversed polarity, and furthermore confirm the presence of an interval of magnetically Reversed polarity spanning an interval of at least 15 million year duration. In addition, we recognize a magnetic overprint of presumed Normal polarity held in antiferromagnetic phases, of presumed Permian age, based on the apparent polar wander path given in Plado et al. (2010).

Introduction

Ever since their discovery nearly 50 years ago, geomagnetic superchrons have been a puzzle for the geophysical community. There have only been a few during Phanerozoic time, and Driscoll and Evans (2016) has recently proposed multiple superchrons during the proterozoic. The two well-studied superchrons are the Cretaceous Long Normal chron (Helsley and Steiner, 1969) and the Kiaman Reversed chron (Irving and Parry, 1963; Kirschvink et al., 2015; McMahon and Strangway, 1968). A third phanerozoic superchron was proposed by Gallet and Pavlov (1996), the Moyero River superchron, which is the study of this paper. Of those that happened during Phanerozoic time, Moyero River superchron is the least-well understood. Initial calibration from Siberia suggested it to be ~ 15 Myr in duration, subsequently revised upward to ~ 20 Myr (Gallet and Pavlov, 1996; Pavlov and Gallet, 2005; Pavlov et al., 2012). The epicontinental sediments of the Moyero region are from the early Paleozoic, but several small gaps exist in the Ordovician record, and the Ordovician/Silurian boundary is missing all together (Gallet and Pavlov, 1996). However, the precise duration of this event has not been calibrated to the conodont biostratigraphic time scale that forms the primary basis of intercontinental correlation for Ordovician time. Plado et al. (2010) and Preeden et al. (2008) previously studied sediments in this area from the lower and middle Ordovician and lower Silurian periods and found a reverse polarity primary component (Dec. 166.0, Inc 56.1), which confirmed the Baltic plate's southern hemisphere location during the Moyero Reverse superchron, but only shows evidence of a reversal in a low temperature secondary component, of supposed younger age, necessitating further study.

The exposed sediments in Estonia are from this time period and are untectonized, which makes it an ideal place to study the Middle Ordovician and thus this superchron. Previous paleomagnetic studies of these rocks show that they generally have very low

magnetic moments and appear to contain multiple overprints from different magnetic minerals, like maghemite, magnetite, and hematite, which make the demagnetization analysis more complex (Preeden et al., 2009). However, new developments in measurement technology have allowed measurement sensitivity to approach that of the SQUID magnetometer system itself. When coupled with proper sample handling to reduce magnetic noise from drilling and handling in lab, samples usually too weak to be accurately measured are now able to provide extensive insight into the history of the magnetic field throughout Earth's history.

Geological Setting

2.1 Tectono-Sedimentary Background

Terrigenous and carbonate sediments ranging from the Ediacaran to the Devonian cover the Svecofennian crystalline basement of the Baltic platform, and those of Ordovician age are exposed on the northern margin of Estonia. The bedrock dips only 8'- 15' (0.13° - 0.25°) to the South over throughout Estonia, excluding local deformation (Preeden et al., 2008). The bedrock is nearly horizontal and thus precludes the use of the usual paleomagnetic tilt test to deduce the timing of magnetic overprints (Enkin, 2003). There is evidence of meteoritic bombardment during the Middle Ordovician, which is coincident with deformation events (Hints, 2014). The majority of the sedimentary rocks formed during the Paleozoic period, and as a result of the slight tilt, the bedrock age decreases to the South. In the northern part of Estonia, the prevailing time period is the Ordovician, whereas the rocks in the southern part of the country are from the Devonian (Meidla, 2014). Estonia's sedimentary record lacks any rocks younger than these, as shown in figure 2. The combination of lacking younger rocks and minimal tilting, it is clear that the Ordovician sequence in Estonia has never been deeply buried nor tectonized. The sediments are thus un-metamorphosed and also contain large amounts of clastic sediments (Plado et al., 2010). Our sampling range covered parts of the Lasnamägi, Aseri, Kunda, and Volkhov stages.

2.2 Middle Ordovician Stages Studied

Estonia's Ordovician sequence is mostly complete has a thickness ranging from 70 to 180 m (Meidla et al., 2014). The stages studied cover the late Dapingian through the middle Darrwilian. The Darrwilian in Estonia ends with the Uhaku stage, which was not studied. The predominate rocks from the investigated locales is limestone that varies in composition

depending on the stage from during which it formed. According to Meidla et al. (2014), the Ordovician limestones formed from cold-water carbonates, which were then deposited in a shallow marine basin. Initially, the basins were sediment starved, but the sedimentation rates have increased upwards in the stratigraphic column.

Lasnamägi is the youngest section studied and consists of partly argillaceous and dolomitized bioclastic limestones (Bauert et al., 2014; Plado et al., 2010). The Aseri stage consists primarily of biomicritic limestone, containing clay-sized particles and ferriferous ooids (Bauert et al., 2014; Hints, 2014). The Kunda stage consists of sandy limestone with kerogene and dolostone inclusions (Hints, 2014; Hints et al., 2012). The Volkhov stage is the oldest section and straddles the Dapingian-Darriwilian boundary (Plado et al., 2010). The stage consists of glauconitic limestones, which have undergone partial to full dolomitization (Hints et al., 2012).

2.3 Biostratigraphy

Conodonts are the best biostratigraphic markers for the Middle Ordovician of the Baltic Platform, whose characteristic fossils first appear in the Volkhov unit. According to Hints et al. (2012), they are well-preserved, giving a temporal resolution of 0.1 Ma. and implying burial temperatures were significantly less than 100°C using the Conodont Alteration Index (Epstein et al., 1977).

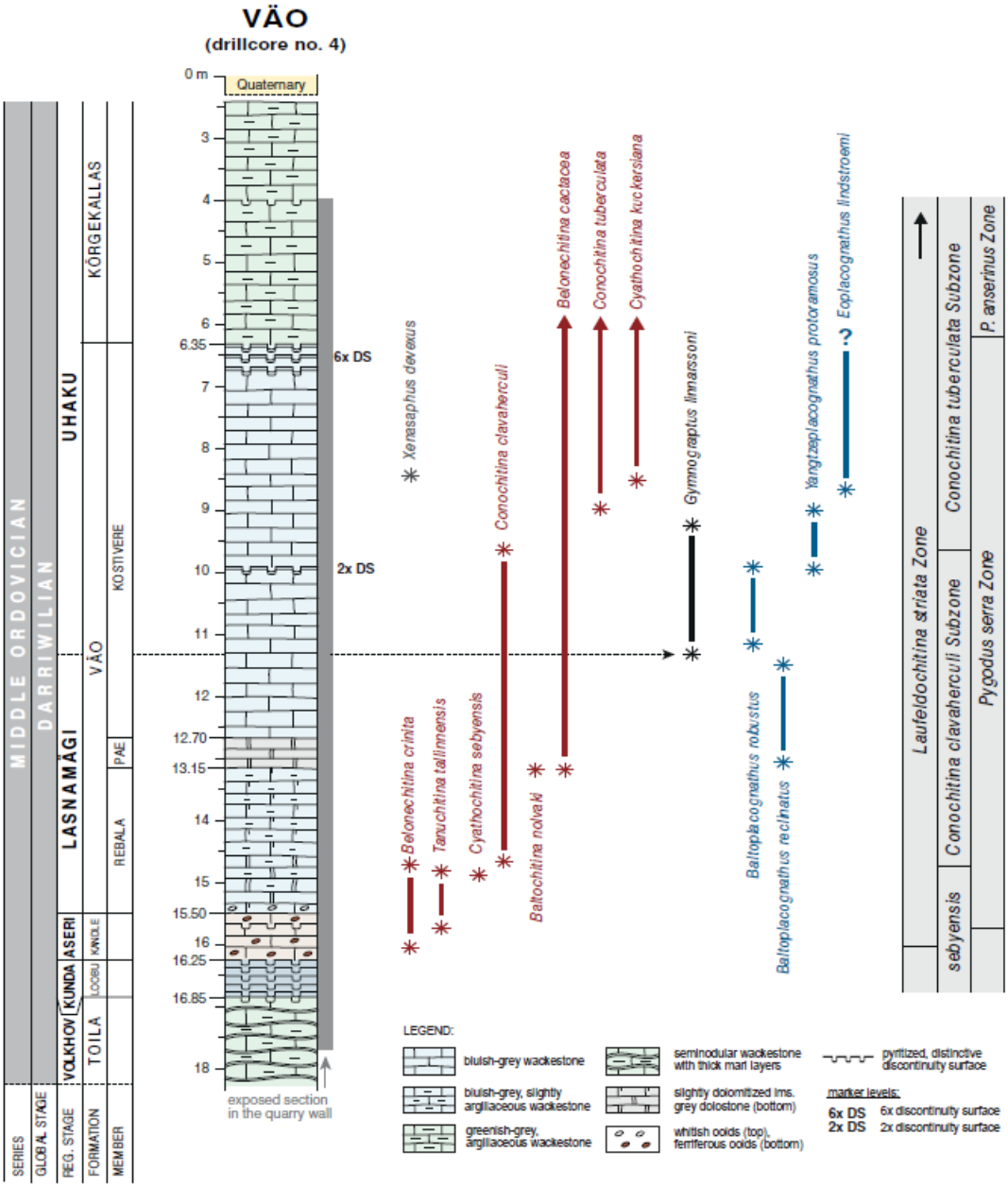

Fig. 1. Biostratigraphy and sedimentary column for Väo quarry, near our sampling sites, showing the various Middle Ordovician stages and their key biostratigraphic taxa. Adapted from Bauert et al. (2014).

Limestone sedimentation rates increase upwards, which correlates well with an increasing rate of carbonate production (Meidla et al., 2014).

2.4 Large-scale geochemistry

As a whole, the sequence is characterized primarily by various limestones that are locally dolomized with occasional thick volcanic interbeds (Meidla, 2014). Northern Estonia is rich in phosphite deposits and, as a result, has numerous quarries throughout the area. In addition, the meteorites from the Middle Ordovician have left behind both shock metamorphic grains and extraterrestrial chromite, in the form of L-condritic chromite grains scattered throughout the country (Hints, 2014; Meidla, 2014).

Sites and rock samples

We studied 3 sites: the Väo quarry near the town of Kunda, and a cliff side near the town of Saka, which are marked on Figure 2. The Väo quarry is an active limestone quarry located near Tallinn and contains rocks ranging in age from the Volkhov stage through the Uhaku stage (Bauert et al., 2014). 15 samples cover 70 cm of its Kunda stage, 11 samples cover 47 cm (all) of the Aseri stage, and 197 samples cover the lower 1456 cm of the Lasnamägi stage. The Kunda locale is also a limestone quarry. Of our samples, 15 covered the upper 83 cm of the Kunda site's Kunda stage, 16 covered 101 cm (all) of the Aseri stage, and 28 cover the bottom 250 of its Lasnamägi stage. The cliff side near Saka had a large amount of limestone from the Middle Ordovician. 37 of our samples covered the upper 236 cm of the locale's Volkhov stage and 15 covered the lower 116 cm of its Kunda stage.

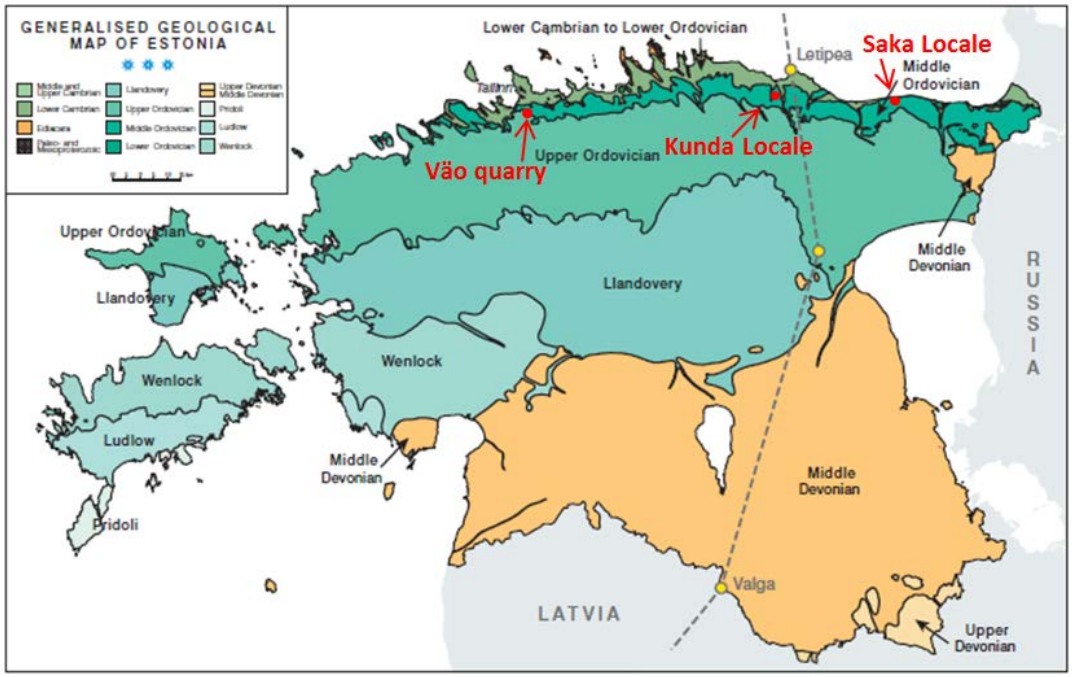

Fig. 2. A generalized geological map of Estonia, showing the Väo quarry, the Kunda locale, and the Saka locale. Adapted from (Meidla, 2014).

From these sites, 306 cylindrical cores (2.5 cm diameter) were drilled using portable gasoline-powered, non-magnetic, diamond-tipped drills. Samples were oriented using standard magnetic and solar compass techniques. Most days on the Baltic Sea were cloudy, so most samples lacked solar compass measurements.

Materials & Methods

For this study, we followed the procedure outlined in Kirschvink et al. (2015) and Kirschvink et al. (2008) due to low volume-normalized magnet moments reported by Plado et al. (2010) and Preeden (2009).

4.1 Sample Preparation

We cut each sample into 1-cm height, 2.54 cm diameter cylinders using a three-bladed diamond-impregnated rock cutting saw. The end chips were saved for later use, and then we labeled the first two 1-cm height samples using non-magnetic, thermal-resistant ink for use in the demagnetization experiments as the .1 and .2 samples, respectively. We then washed the .1 samples in a 12 N HCl solution by dunking them for less than 1s using plastic tongs, and then quickly rinsing with deionized water. The acid reacted with the surface carbonates, removing any trace of metallic contaminants from the drilling and sample preparation procedures, but left the color generally unchanged. We made sure to blow all surfaces clear of dust and debris, and we used disposable, dust-free plastic gloves to handle the samples during the demagnetization and measurement process.

4.2 Paleomagnetism

We conducted remanence measurements on two superconducting rock magnetometers (named Lowenstam and Shoemaker) housed in magnetically shielded rooms on the Caltech campus. Both magnetometers have background instrument sensitivity of around $4 \times 10^{-13}\mathrm{Am}^2$ run in a sham mode without the sample holder. We used 19 mm diameter (1 mm thickness) quartz tubes which were soaked in a 12N HCl acid bath for 3 days before use. During usage, we subjected the empty holders to maximum strength alternating-field (AF)

demagnetization after every 9th sample on Shoemaker and every 6th on Lowenstam. The magnetic moment increased to an average of $2.2 \times 10^{-12}\mathrm{Am}^2$ with the holder installed, with a minimum approaching the machine's resolution. The samples were then taken inside magnetically shielded (< 200 nT) rooms and kept inside for the remainder of the study.

We employed a hybrid demagnetization strategy which has proven effective in the separation of magnetic components on drab-colored, weakly magnetized samples in previous studies (e.g. Ward et al. (1997)). First, we measured the natural remanent magnetization for each sample. Next, we cooled the samples in liquid nitrogen baths for at least 30 minutes at a time to help remove viscous components potentially carried by muti-domain magnetite grains by cycling them through the Verway transition (~ 120 K). We then subjected the samples to alternating-field (AF) demagnetization at field strengths of 2.5 mT, 5.0 mT, and then 7.5 mT with the goal of removing any soft components caused by the transportation or preparation of the samples. Finally, we thermally demagnetized the samples in an inert (N_2) atmosphere, magnetically-shielded oven (< 25 nT net field) in incremental temperature steps (5 °C – 30 °C) steps from 80 °C up to a maximum of 575 °C. We continued the temperature steps on each sample until the sample began to display unusual behavior in its magnetic vector directions. We then determined principle magnetic components using the methods outlined in Kirschvink (1980) and allowed for Maximum Angular Deviations (MAD) of 15°. Similarly to Kirschvink et al. (2015), many samples displayed unusual behavior before reaching the origin or formed stable endpoint clusters, necessitating least-squares circle fits anchored at the origin.

4.3 Rock magnetism

After the initial paleomagnetic analysis, we selected 18 samples (6% of the total number) as representative samples for the rock magnetism study. The samples were selected

taking into account the sampling locale, whether the sample lost magnetic stability at a low (<= 300 °C) or at a high (>= 300 °C) temperature, and during which stage of the Middle Ordovician they formed. Due to the low magnetic moment of the samples, rather than using the front chip for the rockmagnetics survey, the 2nd sample in the core (the .2 sample) was used for the experiments to improve the signal-to-noise ratio. We subjected the to the same rockmagnetic experiments outlined in Kirschvink et al. (2008), including AF progressive demagnetization up to a peak field of 80 mT, followed by the anhysteric remanent magnetization (ARM) Lowrie-Fuller test for single-domain behavior (Johnson et al., 1975). The ARM was acquired progressively using peak AF steps of 100 mT (0-1 mT DC biasing fields). The maximum ARM was then demagnetized using progressive AF. An IRM pulse in a peak field of 100 mT was then applied to the samples, which was then followed by progressive AF demagnetization (Johnson et al., 1975). Progressive IRM experiments were then applied up to 350 mT, which were again followed by progressive AF demagnetization.

Results

5.1 Paleomagnetics

Examples of progressive demagnetization are shown in appendix A for 6 samples. The samples shown represent different stratigraphic sections, blocking temperatures, locales, and overprints. The average magnetization of the samples is given in table 1. After cycling in liquid nitrogen, approximately 3-9% of the NRM intensity was lost, implying the presence of small grains of multi-domain magnetite undergoing a Verway transition. These grains could potentially be the result of the volcanic interbeds or, in a small part, of the Middle Ordovician meteorite bombardment seen in the stratigraphic column, so the lack of a clear direction for the low temperature steps is reasonable.

Table 1
Magnetization values for samples by locale

Locale	NRM (emu)	After LN_2 (emu)	At last coherent step (emu)
Väo (quarry)	7.31×10^{-7}	6.63×10^{-7}	9.59×10^{-8}
Kunda (quarry)	3.76×10^{-6}	3.53×10^{-6}	1.79×10^{-7}
Saka (seaside)	9.49×10^{-7}	9.22×10^{-7}	8.02×10^{-8}

A low blocking temperature component, generally at or below 260 °C, was isolated in 169 of the samples, but in 2 different forms, as shown in figure 3. The directions of all components are given in table 2. In one subset of the samples, this low blocking temperature component showed up as an overprint component,O_L, in a direction around 17° offset from the direction of the current magnetic field. The second form showed up as a primary component, P_w, in samples with a net blocking temperature of less than 260 °C, approximately 12 ° offset from the modern magnetic field direction. This direction, as a primary component, was found only

in samples from the Saka locale, which was also the only seaside locale; the others were quarries. The samples on the sea cliff have undergone more surface weathering, and it makes sense that the more recent component has a lower stability. Due to the flatness of the location, doing a tilt test to help constrain the age of this component is not possible.

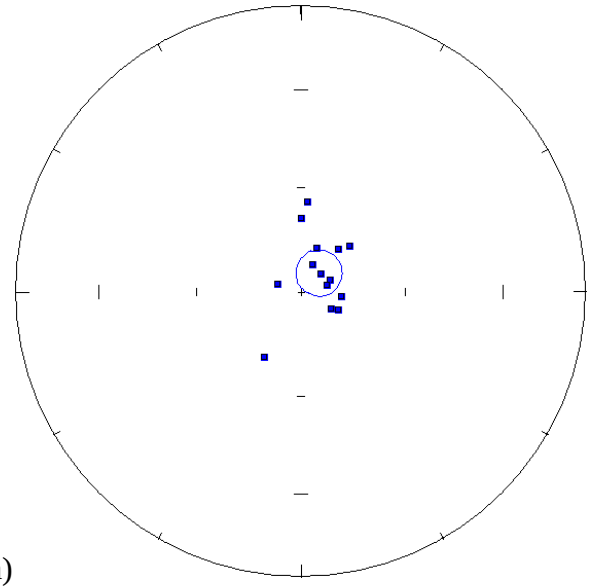

(a)

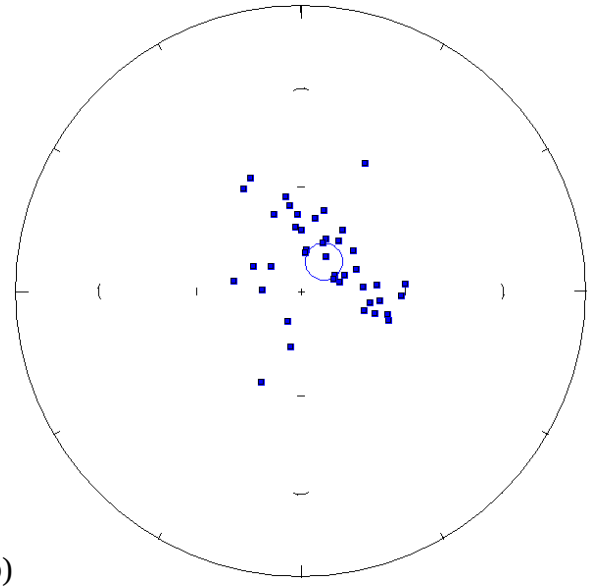

(b)

Fig. 3. The primary direction of low blocking temperature Saka samples in (a) is the same as the low temperature overprint seen in Kunda samples in (b).

Combining all the overprint data yields figure 4, which shows that the average direction of S overall the samples is similar to that of P_w. The number of samples displaying $P_w$is too small to run a paleomagnetic mean direction test, but the angle between the vectors is 6.1°, which is lower than the $\alpha_{95} = 6.6\,^\circ$ for P_w, so the difference in angle does not appear to be sufficient to consider these directions statistically different.

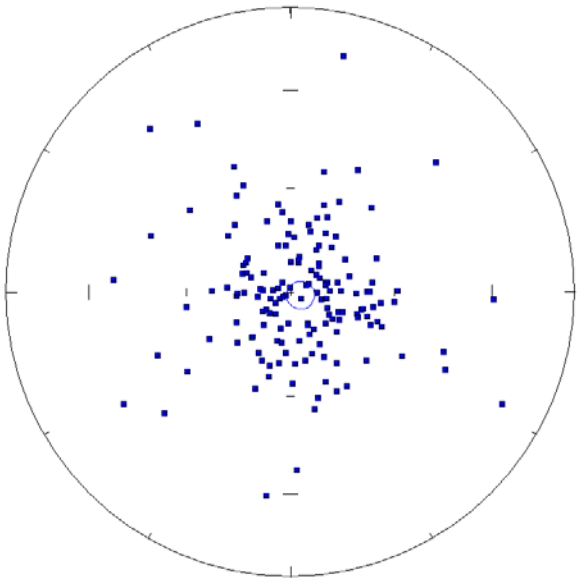

Fig. 4. Average direction of O_L component across all studied samples.

The next component found was the primary component, P, for 130 of the 308 samples and is shown in figure 5. Its direction is consistent with the section being formed in the southern hemisphere during a reversed magnetic chron. The scatter observed is reasonable given the weak NRM of these samples.

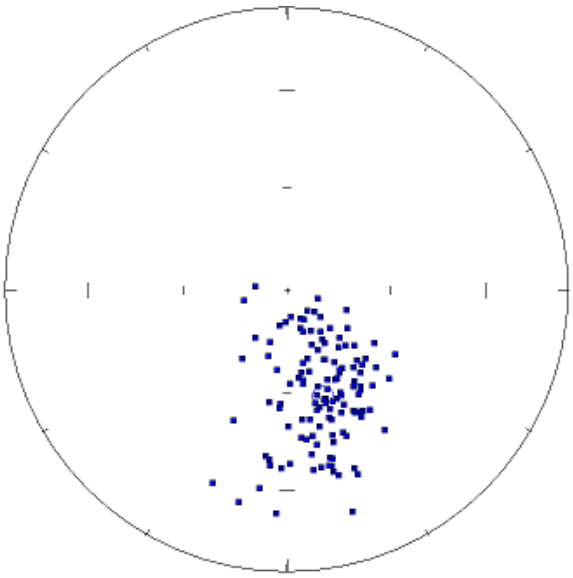

Fig. 5. Average direction of the P component.

The directions of the primary component, of the O_L overprint component, and of the present magnetic field were compared on a stereo plot, shown in figure 6. The plot shows that the directions all lie on the same great circle arc, within their respective errors.

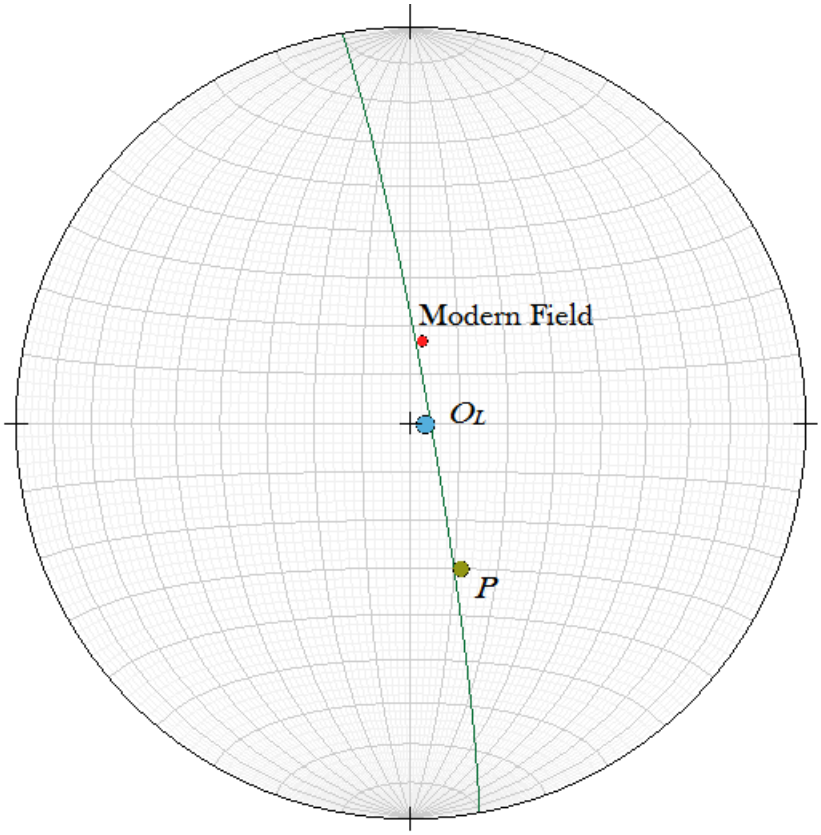

Fig. 6. Stereonet plot showing the modern field, O_L, and P directions.

The co-linearity of the three points in figure 6 means that the overprint is a vector sum of the modern field and the paleofield component, P. Thus, the overprint's origin is most likely the modern field, but the large variability in samples' blocking temperatures (figure 8), however, has prevented the component from being resolved cleanly enough for it to not be statistically different from the modern field.

A high temperature overprint was found in 95 samples using circle fits on samples that had a component in the primary direction but whose demagnetization curves were moving in a direction away from the origin. The intersection of the circle fits gives this overprint's direction. Using these fits was necessary because of the low NRM. For most samples 50-70% of the initial magnetization had already been lost by the first steps that would characterize this component.

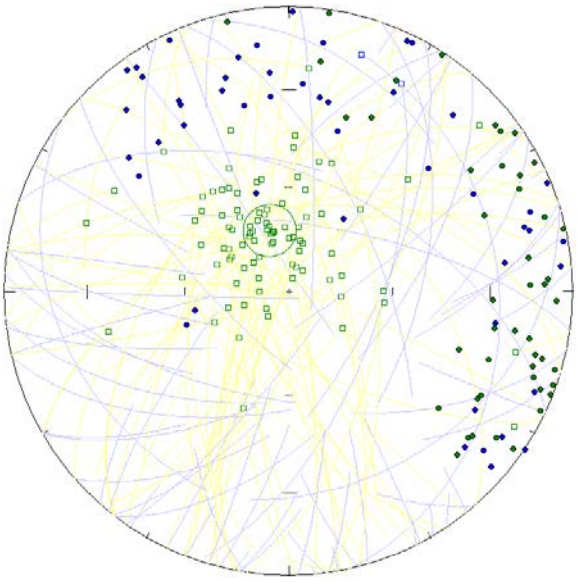

Fig. 7. Circle fits given the mean direction for the O_H component direction.

Running the antiparallel reversals test of the O_H direction against the P direction gives a χ^2 p-value of 0.0003, which means the null hypothesis that the directions are antiparallel can be rejected. Thus, the O_H component is not antipodal of P, which means that $O_H$is a

distinct direction and component. The inclination of this direction is the opposite of that of the modern field, so the direction of O_H is distinct from the modern field's direction.

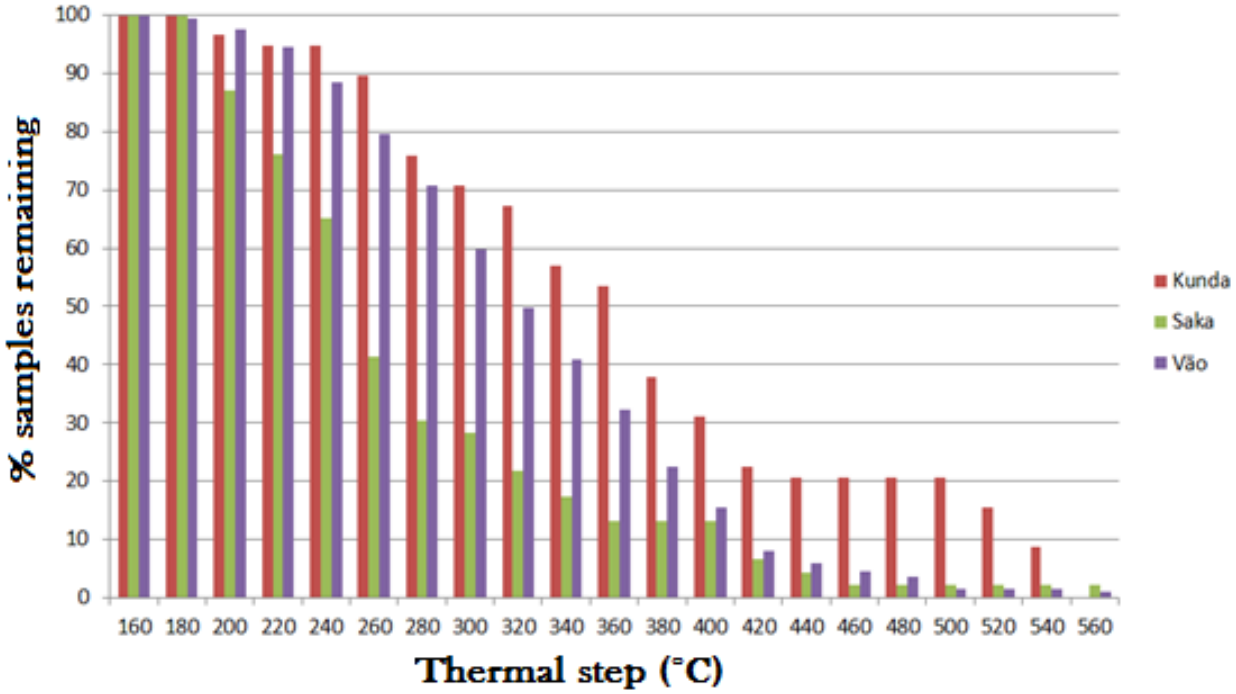

Fig. 8. Survivorship histogram for the primary components for samples from all three locales.

Most samples lost coherency by 500 °C, and the few that reached higher temperatures were mostly found in the Kunda locale. The samples from the Saka cliffs show a clear drop in number of samples from 240 to 260 °C, but then levels off somewhat at 360 °C and above for the more stable samples. This behavior is reasonable given the $P_w$direction found in some of the Saka samples. The samples from the Kunda locale generally were the strongest and also have the highest blocking temperatures. The Väo section was the largest and shows a generally linear decrease from 240 °C to 400 °C, which is reasonable for weak samples.

Table 2

Paleomagnetic results from Estonian Middle Ordovician samples reported in this study. Dec. = declination; Inc. = inclination; κ = Fisher's precision parameter; α_{95} = 95% confidence cone

Components	N	Dec.	Inc.	κ	R	$\alpha 95$
P	130	161.2	57.7	53.9	127.6	2.8
P_w	14	43.8	82.5	212.1	13.9	6.6
O_L	169	95.9	86.9	8.5	149.2	3.7
O_H	47.5	342.5	-71.8	7.3	41.2	7.5

5.2 Rockmagnetics

Once we finished the thermal steps, these data were used to select the 18 samples that underwent the rockmagnetic survey in order to try to better constrain the minerals responsible for the various magnetic directions measured. Figure 9 shows the result of the Lowrie-Fuller test for sample Kun-20.2 to determine the configuration of the sample's magnetic domains.

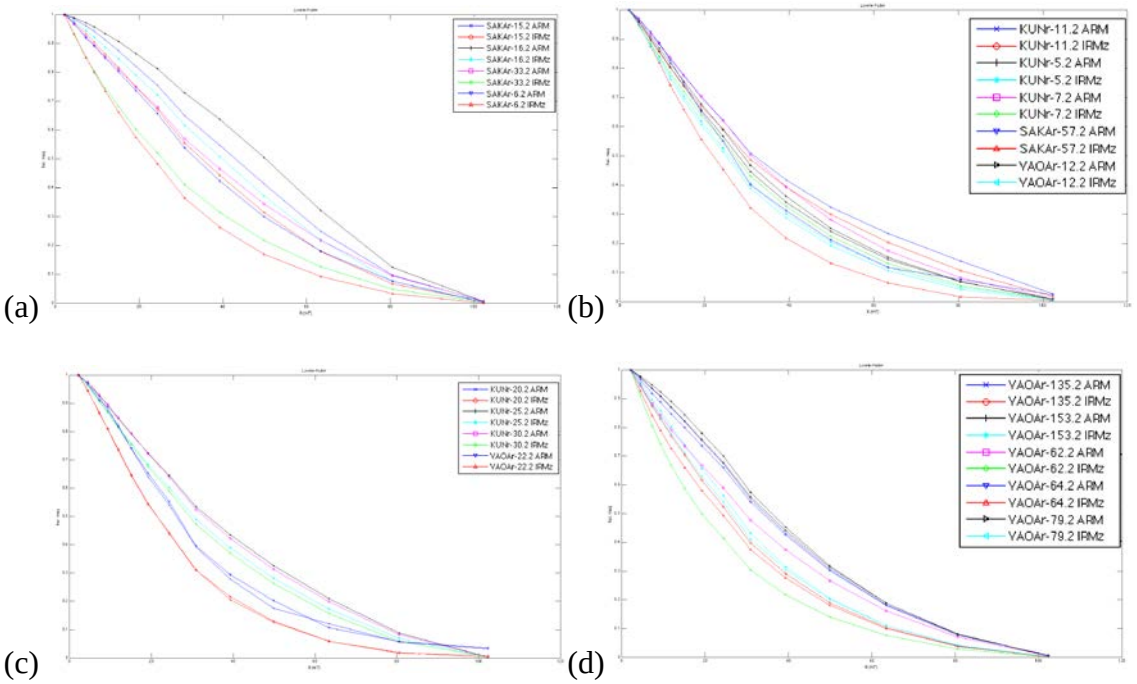

Fig. 9. Lowrie-Fuller tests seen in the studied samples (a) Volkhov, (b) Kunda, (c) Aseri, and (d) Lasnamägi stratigraphic sections. All show single domain crystals.

The ARM curve's position above the IRMz curve for their entire length is

characteristic of single domain crystals (Dunlop, 1972). This result is the same for every sample surveyed.

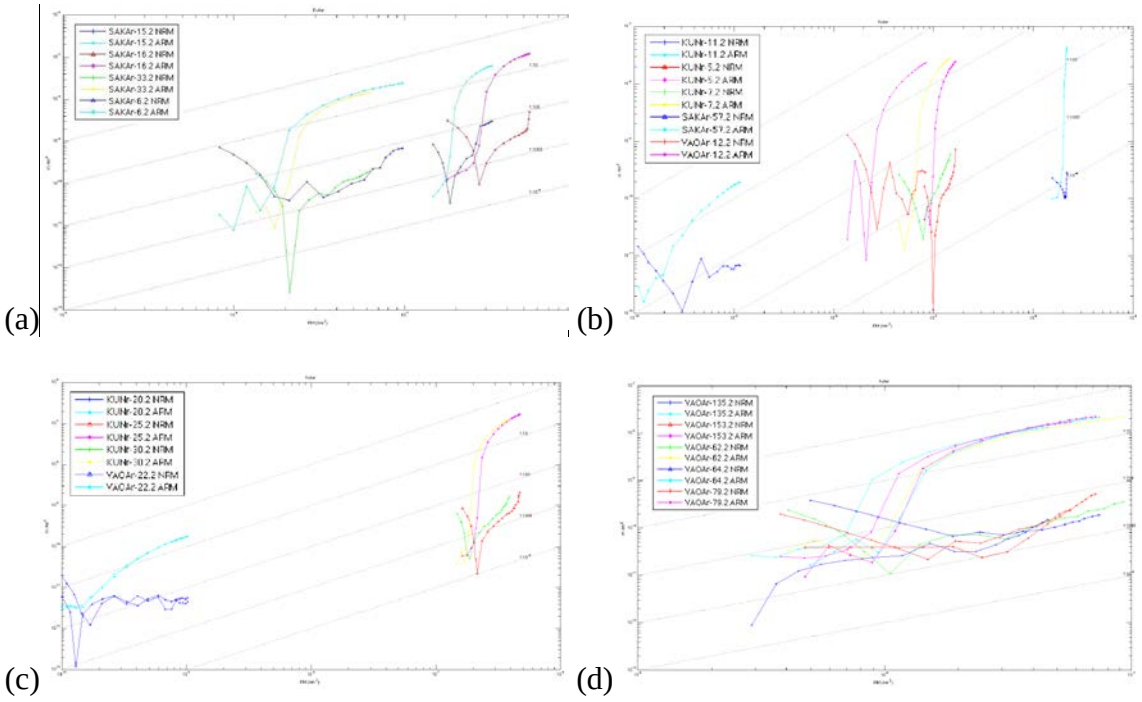

Fig. 10. Fuller test characteristic of the samples studied; (a) Volkhov, (b) Kunda, (c) Aseri, and (d) Lasnamägi stratigraphic sections. All sections show a detrital origin.

Figure 10 shows the results from the Fuller test (Fuller et al., 2002). This test characterizes the origin of the sample's remnant magnetization. The NRM line is located approximately two orders of magnitude below the ARM line. The result found is characteristic of detrital magnetism, which makes sense given that the samples are made of limestone and are weakly magnetized. Every sample studied had this same signature.

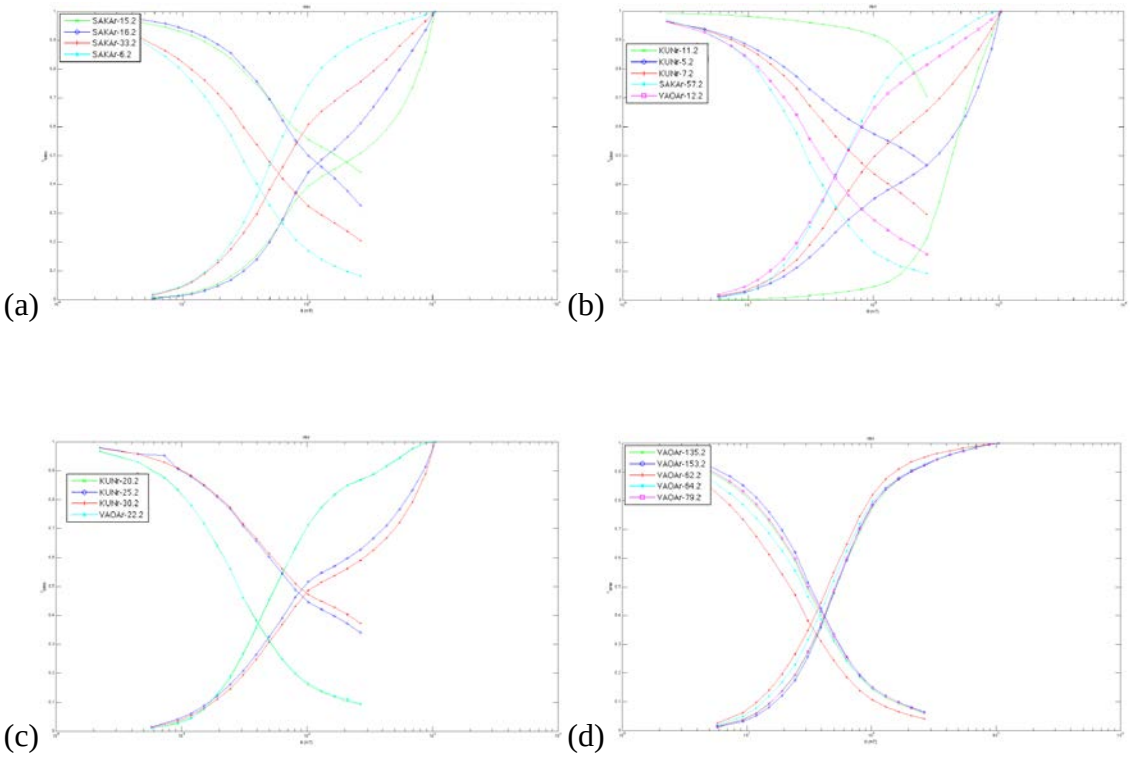

Fig. 11. IRM acquisition curve types seen in the studied sections; (a) Volkhov, (b) Kunda, (c) Aseri, and (d) Lasnamägi stratigraphic sections.

The IRM acquisition curves in figure 11 for samples VAO-62.2 and SAKA-15.2 are characteristic of the two types of curves that were found. The former is characteristic of magnetite and the latter is characteristic of a sample with an additional, high coercivity mineral present, like hematite (Cisowski, 1981). Curves whose tails tapered off at high $\boldsymbol{B}$ were found in samples with blocking temperatures below 300 °C or ones that only exhibited the P component. Curves with similar shapes to the latter were found for samples that exhibited the presence of O_H or had blocking temperatures above 340 °C. The samples generally had $H_{cr} \in (32.5\,, 49.7)$ mT, but some had H_{cr} values up to 440.4 mT. Accordingly, these samples also had stronger high coercivity peaks in figure 13.

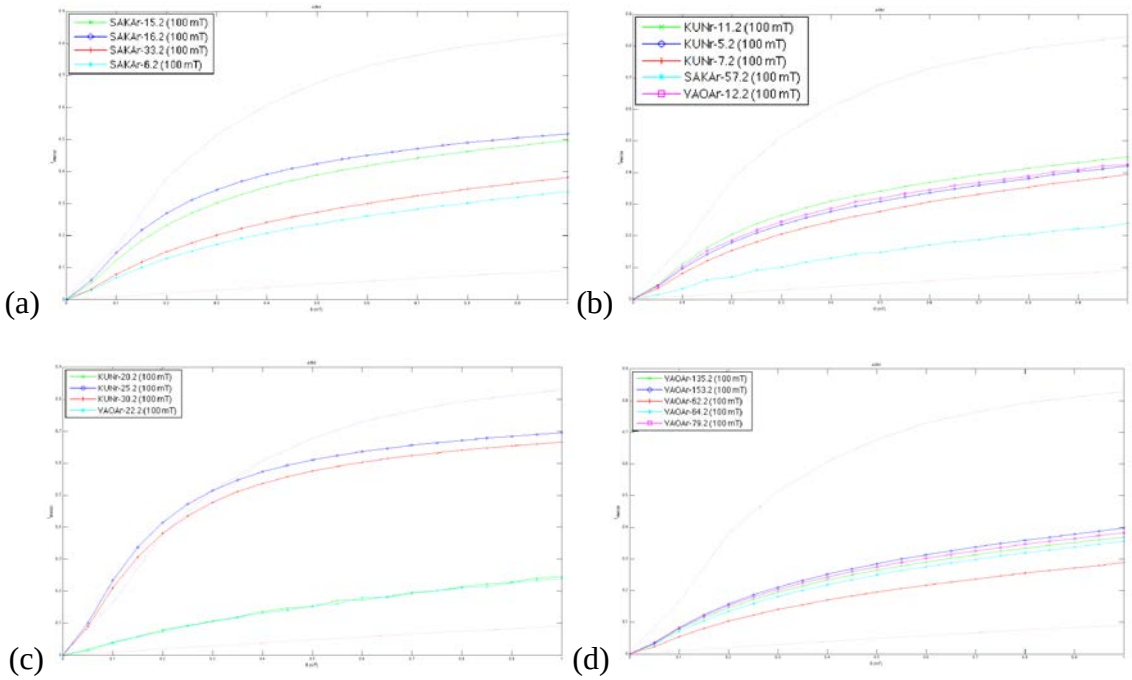

Fig. 12. ARM curves selected to represent (a) Volkhov, (b) Kunda, (c) Aseri, and (d) Lasnamägi stratigraphic sections. The interactivity generally increases up the stratigraphic column, but the Aseri section has strange bimodal behavior.

The ARM curves in figure 12 are divided up by stratigraphic section. The upper reference line is for non-interacting domains, and the lower reference line is for highly interacting domains (Kobayashi et al., 2006). There is a general trend that the magnetic grains become more interacting as the section's age decreases. The most variability, however, is seen in the Aseri section, where the data is bimodal. The samples with strongly interacting grains also showed smaller peaks in the dIRM/dB curves around $\log(B) = 2.5$. There does not appear to be a correlation with blocking temperature.

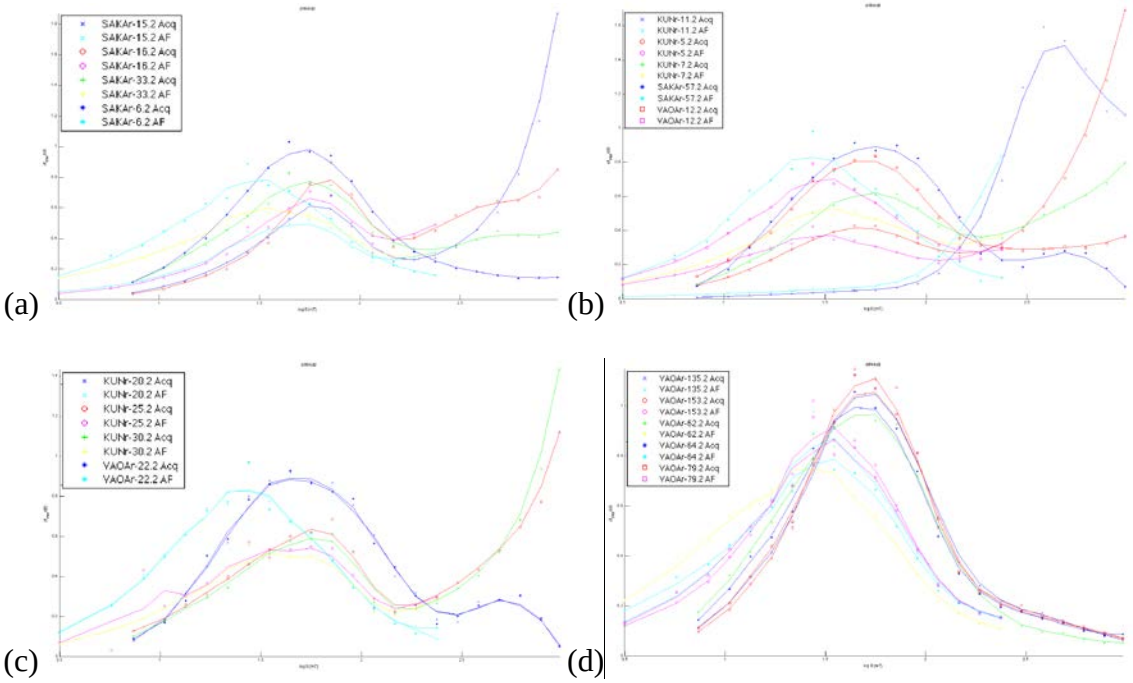

Fig. 13. dIRM/dB curves selected to represent (a) Volkhov, (b) Kunda, (c) Aseri, and (d) Lasnamägi stratigraphic sections. These curves show more variation than other data found in the rockmagnetic study but are well-correlated with stratigraphic section.

The dIRM/dB curves in figure 13 are again divided by section. The peak near $\log(B) = 1.8$ is characteristic of magnetite, and it appears to be the primary component (Peters and Dekkers, 2003). Samples from the Volkhov, Aseri, and Kunda stratigraphic sections show clear evidence of a high coercivity component, shown by the peak (or upward trend, due to equipment limitations) at $\log(B) > 2.5$. This peak, however, is absent from Lasnamägi samples.

Discussion

The previous work in this area reported a primary component and secondary component exhibiting both normal and reversed polarities. Our study found a primary component in a similar direction to Plado et al. (2010)'s P_{DD} direction (Dec. 166.0, Inc. 56.1), which corresponds to the same geologic strata as our samples. Running a parallel reversals test shows that we cannot reject the null hypothesis that our P and their P_{DD} have the same direction. Their data also showed a high coercivity secondary component, which like the one we measured appears to be carried by hematite. Our O_H direction is statistically distinct from that reported in Plado et al. (2010), but the samples that demonstrated this high coercivity overprint in their study include samples outside our study range. The maximum blocking temperature recorded for a sample demonstrating the P component was 575 °C, the most likely carrier for this carrier is magnetite, which agrees with their result.

As the low temperature overprint, O_L, loses coherency at temperatures around 260 °C, the most likely carriers for this component are either pyrrohite or maghemite. Maghemite seems the most likely because it usually is the product of weathering magnetite, and the more highly weathered rocks (with component P_W) from the Saka cliff show a similar blocking temperature to O_L in both the quarry rocks and Saka samples with a higher blocking temperature.

In 95 of the samples, the vector directions veer away from the origin at high thermal steps. Fitting this off-origin trend with circle fit to try to infer the final linear component of the samples yielded the high temperature overprint, O_H. It does not have a clear blocking temperature, and the highest temperature any sample reached was below the Curie temperature of magnetite. The most probable carrier for this component is an antiferromagnetic mineral like hematite, instead of a ferrimagnetic mineral. However, the

hematite peak is consistently missing in samples from the Lasnamägi strata, which contains a large number of the samples displaying O_H.

In none of the components did we find a reversal, unlike in Gallet and Pavlov (1996). This may be the result of the samples being too weak or a lack of deposition in the area during the relatively short normal period that ended the superchron. The Middle Ordovician spans approximately 13 Myr (~470 Ma to ~458 Ma), but our samples do not cover the Uhaku stage, the youngest Middle Ordovician stage in Estonia. Our samples cover less than 10 Myr, so they are insufficient by themselves to determine the boundaries of the superchron. Opdyke and Channell (1996) reported the presence of multiple reversals, with predominating normal polarity, during the Middle Ordovician. We found only reversed polarity component, supporting Pavlov and Gallet (2005), who notes that the difference may be the result of a different Cambrian/Ordovician boundary definition. The Moyero Reverse Superchron starts in the lower Ordovician (approximately 10 Myr before the Darriwilian), so the lack of reversals found through the local Lasnamägi stage in these samples helps to give further evidence to the superchron existing and its length being over 15 Myr, as updated in (Pavlov and Gallet, 2005).

Acknowledgements

We thank Valerie Pietrasz for help with sample preparation and moral support throughout the data collection process.

References

Bauert, H., Einasto, R., and Nõlvak, J., 2014, Stop A5: Väo quarry: 4th Annual Meeting of IGCP 591, v. Field Guide, p. 151-154.

Cisowski, S., 1981, INTERACTING VS NON-INTERACTING SINGLE DOMAIN BEHAVIOR IN NATURAL AND SYNTHETIC SAMPLES: Physics of the Earth and Planetary Interiors, v. 26, no. 1-2, p. 56-62.

Driscoll, P. E., and Evans, D. A. D., 2016, Frequency of Proterozoic geomagnetic superchrons: Earth and Planetary Science Letters, v. 437, p. 9-14.

Dunlop, D. J., 1972, MAGNETIC MINERALOGY OF UNHEATED AND HEATED RED SEDIMENTS BY COERCIVITY SPECTRUM ANALYSIS: Geophysical Journal of the Royal Astronomical Society, v. 27, no. 1, p. 37-&.

Enkin, R. J., 2003, The direction-correction tilt test: an all-purpose tilt/fold test for paleomagnetic studies: Earth and Planetary Science Letters, v. 212, no. 1-2, p. 151-166.

Epstein, A. G., Epstein, K. L., and Harris, L. D., 1977, Conodont color alteration - an index to organic metamorphism: Geological Society of America Special Paper, v. 153, p. 108.

Fuller, M., Kidane, T., and Ali, J., 2002, AF demagnetization characteristics of NRM, compared with anhysteretic and saturation isothermal remanence: an aid in the interpretation of NRM: Physics and Chemistry of the Earth, v. 27, no. 25-31, p. 1169-1177.

Gallet, Y., and Pavlov, V., 1996, Magnetostratigraphy of the Moyero river section (north-western Siberia): Constraints on geomagnetic reversal frequency during the early Palaeozoic: Geophysical Journal International, v. 125, no. 1, p. 95-105.

Helsley, C. E., and Steiner, M. B., 1969, EVIDENCE FOR LONG INTERVALS OF NORMAL POLARITY DURING CRETACEOUS PERIOD: Earth and Planetary Science Letters, v. 5, no. 5, p. 325-&.

Hints, O., 2014, Stop A1: Pakerort and Uuga Cliffs on the Pakri Peninsula: 4th Annual Meeting of IGCP 591, v. Field Guide, p. 133-137.

Hints, O., Viira, V., and Nolvak, J., 2012, Darriwilian (Middle Ordovician) conodont biostratigraphy in NW Estonia: Estonian Journal of Earth Sciences, v. 61, no. 4, p. 210-226.

Irving, E., and Parry, L. G., 1963, THE MAGNETISM OF SOME PERMIAN ROCKS FROM NEW-SOUTH-WALES: Geophysical Journal of the Royal Astronomical Society, v. 7, no. 4, p. 395-411.

Johnson, H. P., Lowrie, W., and Kent, D. V., 1975, STABILITY OF ANHYSTERETIC REMANENT MAGNETIZATION IN FINE AND COARSE MAGNETITE AND MAGHEMITE PARTICLES: Geophysical Journal of the Royal Astronomical Society, v. 41, no. 1, p. 1-10.

Kirschvink, J. L., 1980, THE LEAST-SQUARES LINE AND PLANE AND THE ANALYSIS OF PALEOMAGNETIC DATA: Geophysical Journal of the Royal Astronomical Society, v. 62, no. 3, p. 699-718.

Kirschvink, J. L., Isozaki, Y., Shibuya, H., Otofuji, Y., Raub, T. D., Hilburn, I. A., Kasuya, T., Yokoyama, M., and Bonifacie, M., 2015, Challenging the sensitivity limits of Paleomagnetism: Magnetostratigraphy of weakly magnetized Guadalupian-Lopingian (Permian) Limestone from Kyushu, Japan: Palaeogeography Palaeoclimatology Palaeoecology, v. 418, p. 75-89.

Kirschvink, J. L., Kopp, R. E., Raub, T. D., Baumgartner, C. T., and Holt, J. W., 2008, Rapid, precise, and high-sensitivity acquisition of paleomagnetic and rock-magnetic data:

Development of a low-noise automatic sample changing system for superconducting rock magnetometers: Geochemistry Geophysics Geosystems, v. 9.
Kobayashi, A., Kirschvink, J. L., Nash, C. Z., Kopp, R. E., Sauer, D. A., Bertani, L. E., Voorhout, W. F., and Taguchi, T., 2006, Experimental observation of magnetosome chain collapse in magnetotactic bacteria: Sedimentological, paleomagnetic, and evolutionary implications: Earth and Planetary Science Letters, v. 245, no. 3-4, p. 538-550.
McMahon, B. E., and Strangway, D. W., 1968, INVESTIGATION OF KIAMAN MAGNETIC DIVISON IN COLORADO REDBEDS: Geophysical Journal of the Royal Astronomical Society, v. 15, no. 3, p. 265-&.
Meidla, T., 2014, Estonia - a Palaeozoic country: 4th Annual Meeting of IGCP 591, v. Field Guide, p. 111-113.
Meidla, T., Ainsaar, L., and Hints, O., 2014, The Ordovician System in Estonia: 4th Annual Meeting of IGCP 591, v. Field Guide, p. 116-122.
Opdyke, N., and Channell, J., 1996, Magnetic stratigraphy: Academic, San Diego.
Pavlov, V., and Gallet, Y., 2005, A third superchron during the Early Paleozoic: Episodes, v. 28, no. 2, p. 78-84.
Pavlov, V. E., Veselovskiy, R. V., Shatsillo, A. V., and Gallet, Y., 2012, Magnetostratigraphy of the Ordovician Angara/Rozhkova River section: Further evidence for the Moyero reversed superchron: Izvestiya-Physics of the Solid Earth, v. 48, no. 4, p. 297-305.
Peters, C., and Dekkers, M. J., 2003, Selected room temperature magnetic parameters as a function of mineralogy, concentration and grain size: Physics and Chemistry of the Earth, v. 28, no. 16-19, p. 659-667.
Plado, J., Preeden, U., Pesonen, L. J., Mertanen, S., and Puura, V., 2010, Magnetic history of Early and Middle Ordovician sedimentary sequence, northern Estonia: Geophysical Journal International, v. 180, no. 1, p. 147-157.
Preeden, U., 2009, Remagnetizations in sedimentary rocks of Estonia and shear and fault zone rocks of southern Finland [Doctor of Philosophy: University of Tartu, 52 p.
Preeden, U., Mertanen, S., Elminen, T., and Plado, J., 2009, Secondary magnetizations in shear and fault zones in southern Finland: Tectonophysics, v. 479, no. 3-4, p. 203-213.
Preeden, U., Plado, J., Mertanen, S., and Puura, V., 2008, Multiply remagnetized Silurian carbonate sequence in Estonia: Estonian Journal of Earth Sciences, v. 57, no. 3, p. 170-180.
Ward, P. D., Hurtado, J. M., Kirschvink, J. L., and Verosub, K. L., 1997, Measurements of the Cretaceous paleolatitude of Vancouver Island: Consistent with the Baja British Columbia hypothesis: Science, v. 277, no. 5332, p. 1642-1645.

Appendix

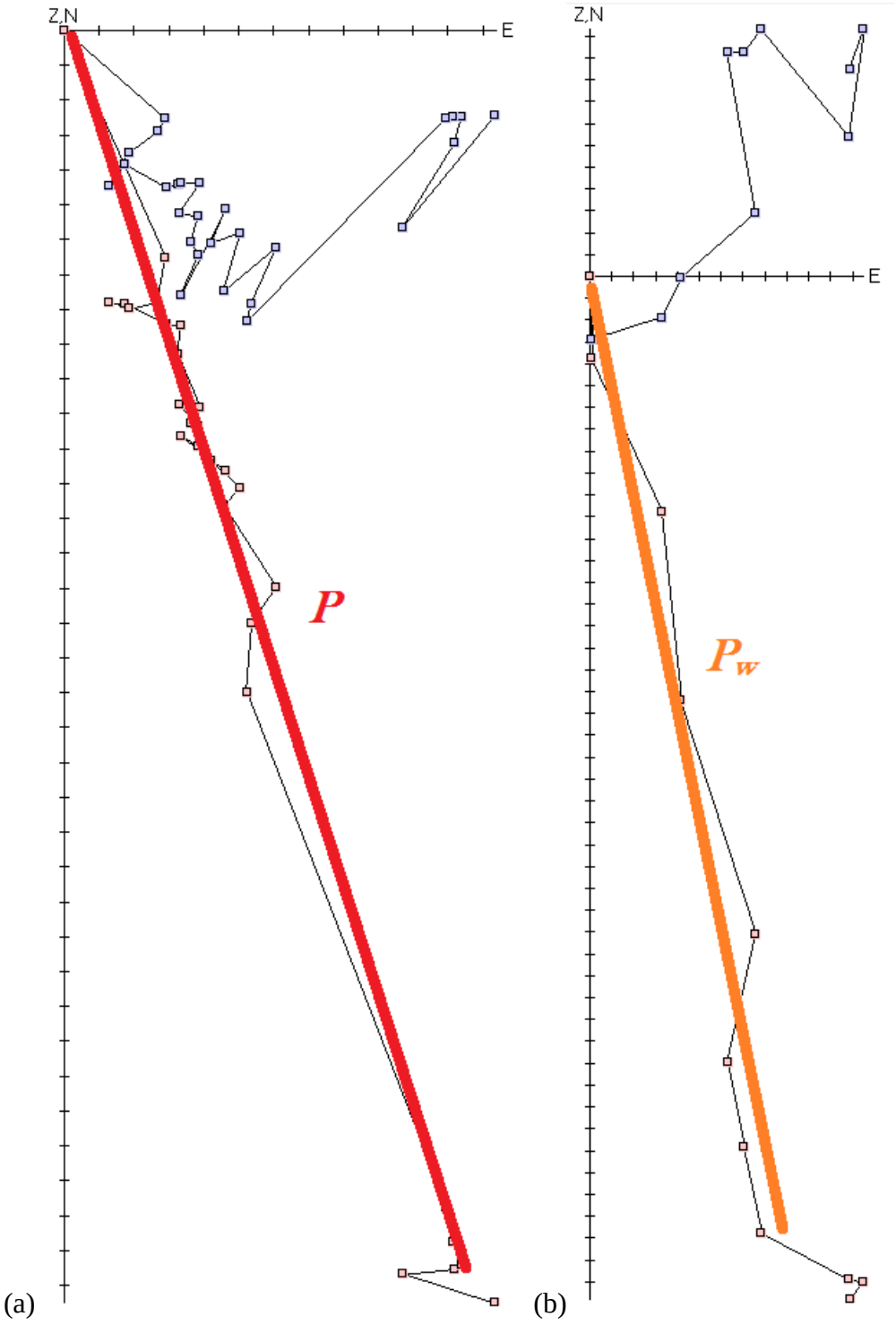

Fig. A1. Zijdervelds for samples SAKA-16.1 (a) and SAKA-22.1 (b).

Both samples in Figure A1 are from the cliff side near Saka, Estonia. Sample SAKA-16.1's Zijderveld appears to lack any clear overprint directions. It had a blocking temperature of 575 °C, among the highest of the samples investigated. Its main direction is

the *P* direction found throughout the sections investigated. Sample SAKA-22.1's Zijderveld has a similar shape to that of the former sample, but its magnetic field vectors lost cohesion after many fewer steps, at 260 °C. Both samples are from the Volkhov stratigraphic section.

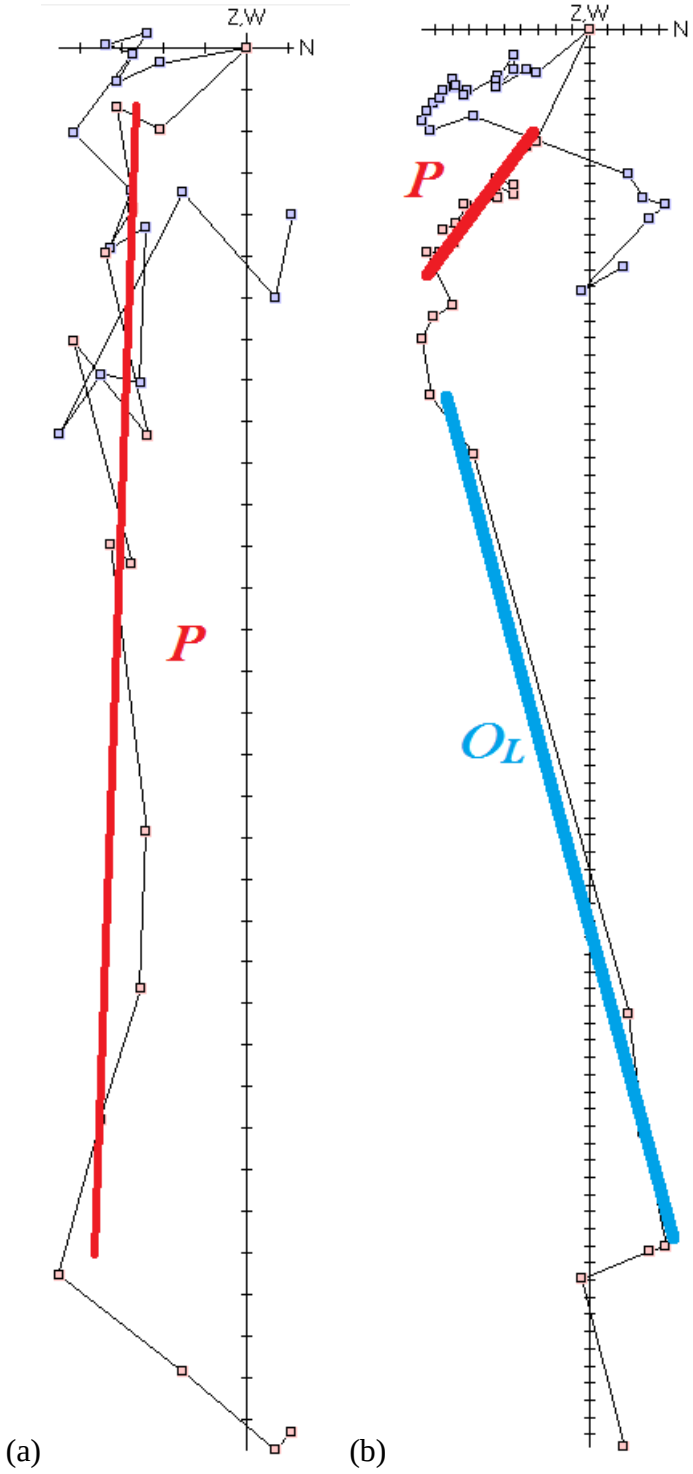

Fig. A2. Zijdervelds for samples KUN-3.1 and KUN-27.1

Figure A2 shows 2 example samples from the quarry near Kunda, Estonia. Sample KUN-3.1 demonstrates some of the weird paths that the Zijdervelds travelled on the way to the origin, which helps explain why the data have large errors. The blocking temperature of this sample was intermediate, at 300 °C, so the lack of an O_L direction is reasonable. Sample KUN-27.1 shows a clear O_L direction, in addition to the P direction. Its blocking temperature was on the higher end, at 500 °C. The former sample is from the Kunda stratigraphic section, and the latter sample is from the Aseri section.

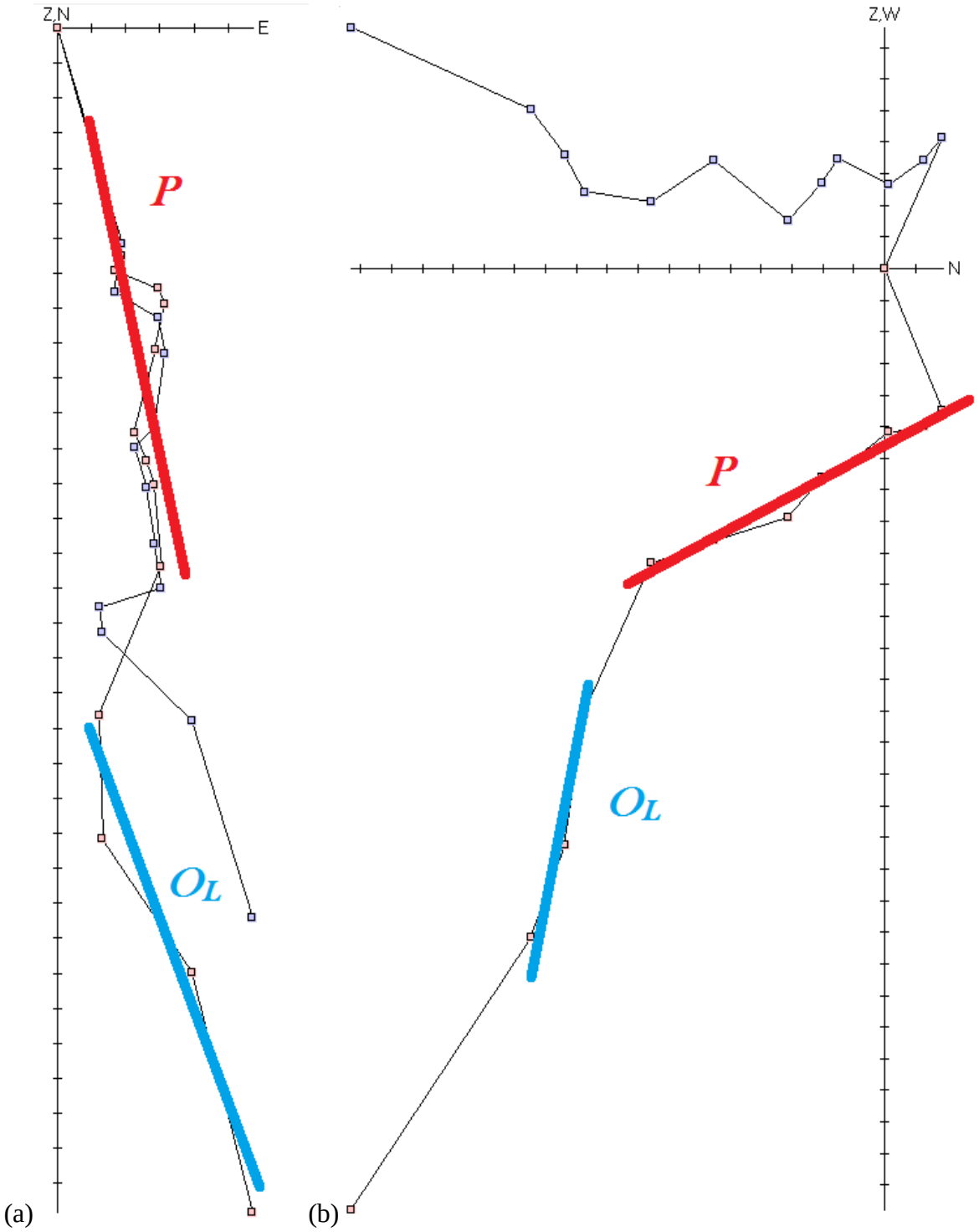

Fig. A3. Zijdervelds for samples VAO-114.1 (a) and VAO-209.1 (b)

Both samples in figure A3 are from the Väo quarry, are from the Lasnamägi stratigraphic section, and show both the O_L and P directions. Sample VAO-114.1 had a blocking temperature of 320 °C, and sample VAO-209.1 had a blocking temperature of 300 °C. The magnetic vector line for sample VAO-209.1 clearly is going in a direction away

from the origin, but like many samples, it lost cohesion before the O_H overprint could be determined.

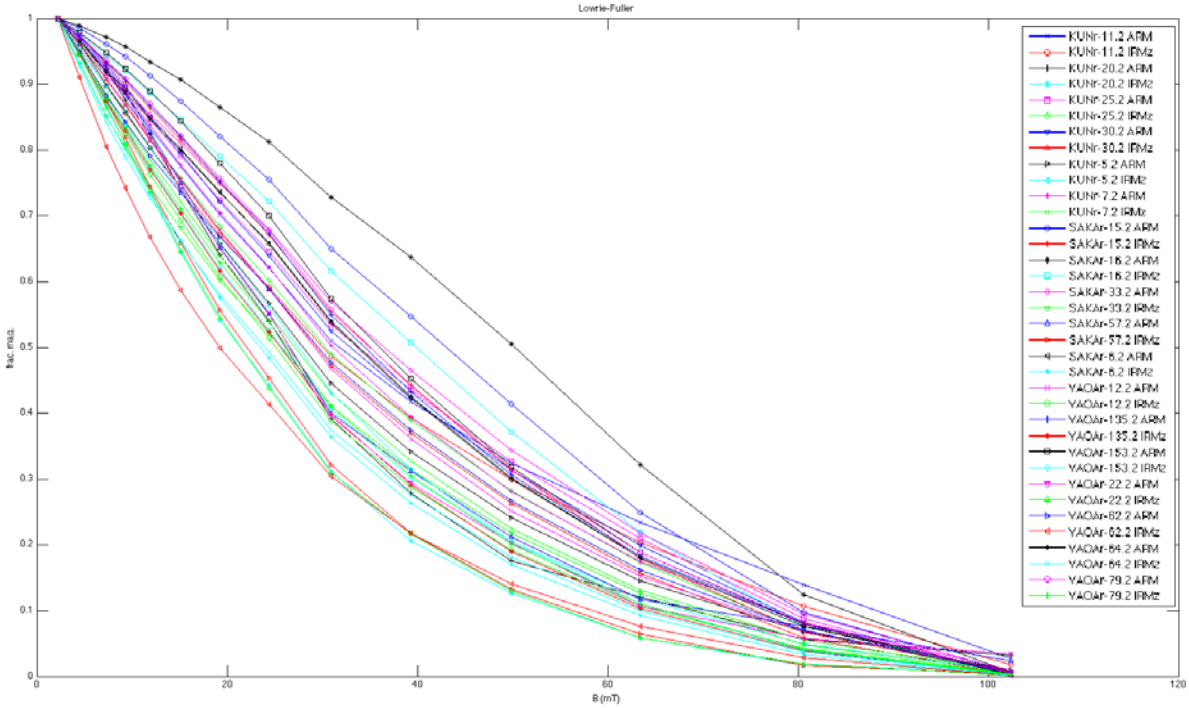

Fig. A4. Lowrie-Fuller test for all samples studied.

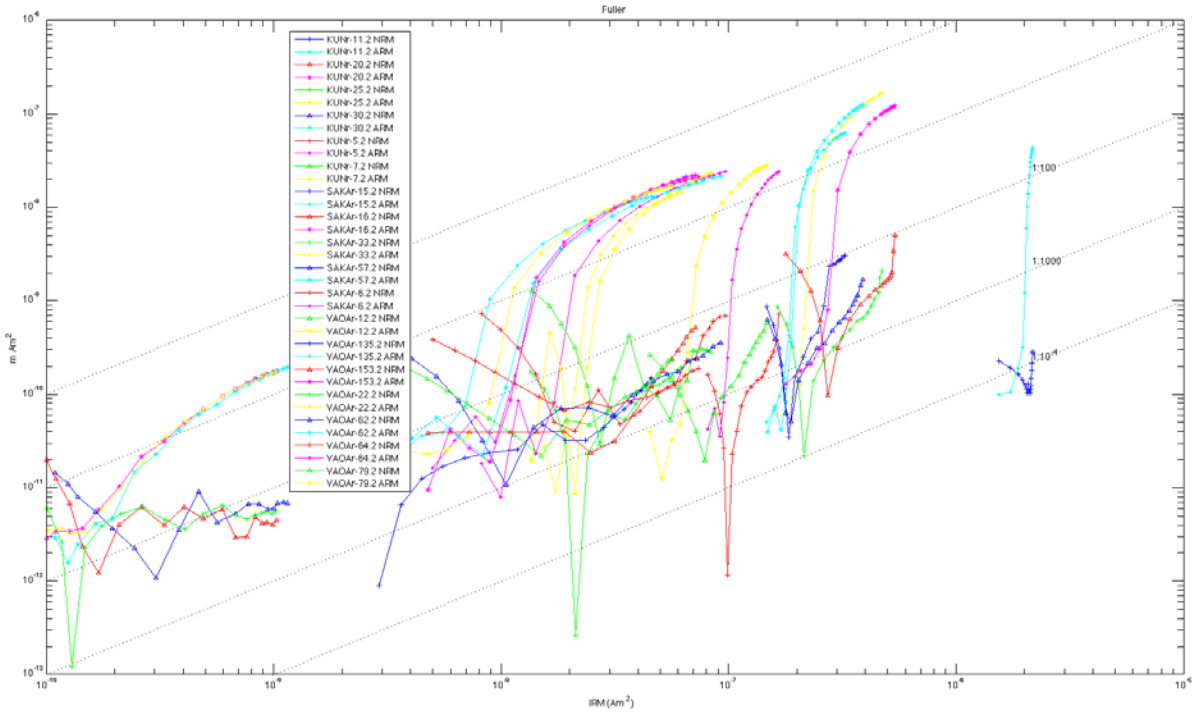

Fig. A5. Fuller test for all samples studied.

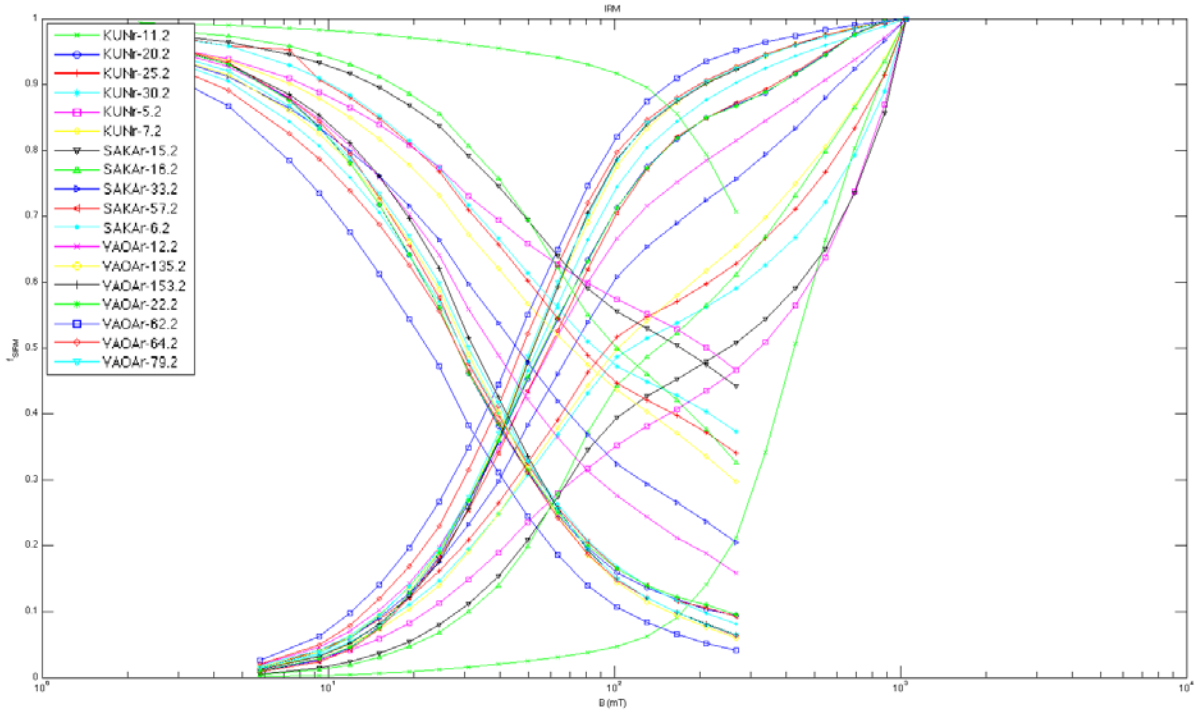

Fig. A6. IRM acquisition curves for all samples studied.

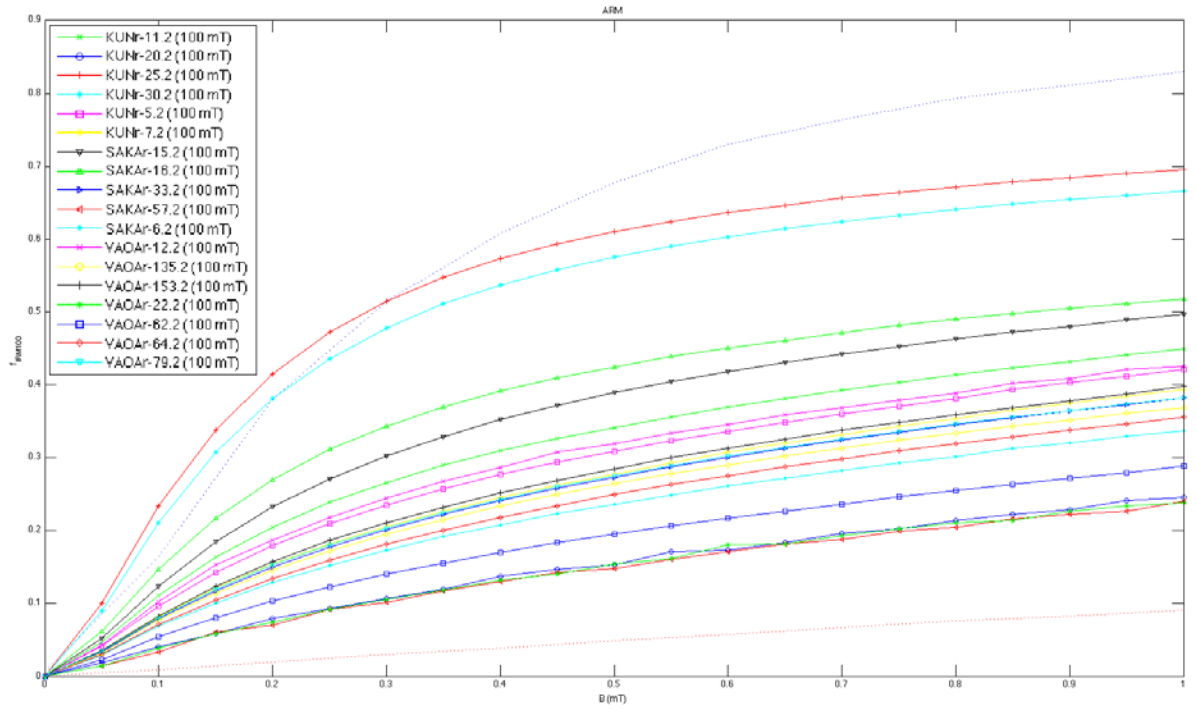

Fig. A7. ARM curves for all samples studied.

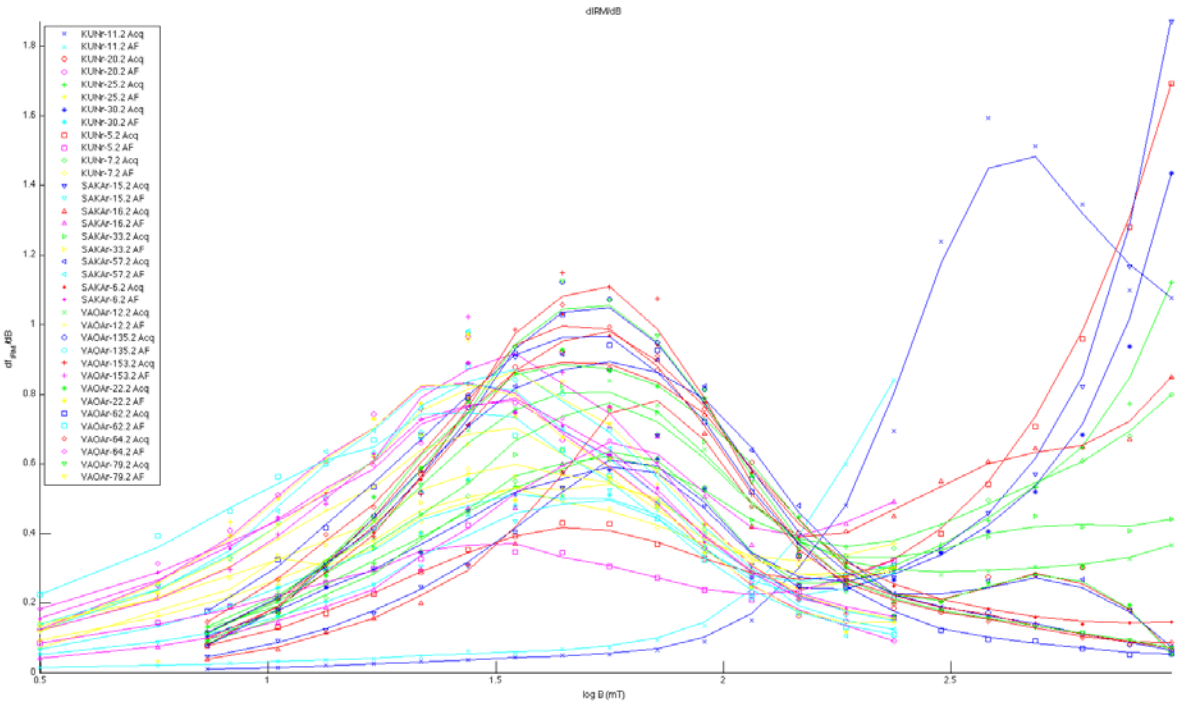

Fig. A8. dIRM/DB curves for all samples studied.